JOURNAL OF CATALYSIS **81,** 95–106 (1983)

Interaction of HCOOH with a Rhodium Surface, Studied by Auger Electron, Electron Energy Loss, and Thermal Desorption Spectroscopy

F. SOLYMOSI[1] AND J. KISS

Reaction Kinetics Research Group, The University, PO Box 105, Szeged, Hungary

Received July 27, 1982; revised November 3, 1982

The interaction of HCOOH with Rh foil has been investigated by various techniques at low and high temperatures with the primary motivation to determine the stability of formate species on unsupported Rh. The electron energy loss spectrum of Rh foil in the electronic range exhibited losses at 4.1, 5.4, 19.6, and 29.5 eV. Adsorption of HCOOH on Rh at 95 K produced new losses at 8.2, 11.3, and 14.2 eV. The intensities of these losses decreased with rise of sample temperature, and new losses developed at 9.5 ($O_{(a)}$) and 13.2 eV ($CO_{(a)}$). On the basis of the behaviour of the above losses, as well as that of the observed decomposition/desorption products of adsorbed HCOOH, it is concluded that (i) HCOOH is adsorbed dissociatively on Rh even at ~100 K, producing adsorbed H and formate species, (ii) the surface formate starts to decompose slightly below 200 K yielding H_2, CO_2, chemisorbed CO, and O, (iii) the decomposition goes to completion around 300 K, and (iv) the primary products of decomposition of formate species strongly interact with the Rh surface.

1. INTRODUCTION

In studies of the surface interactions $H_2 + CO_2$ and $H_2 + CO$ on alumina, magnesia, and titania-supported Rh, we identified the formation of surface formate ion at 300–473 K by infrared spectroscopic measurements (*1–4*). The ir spectra obtained were the same as those observed during the adsorption of HCOOH on these samples. Although no formation of formate ion occurred in the $H_2 + CO_2$ and $H_2 + CO$ interactions on the supports alone, i.e., without Rh under otherwise similar conditions, there was strong evidence that formate ion is most probably located not on the Rh, but rather on the support. However, as the vibration frequencies of formate ion are almost the same on different solids (the positions of the bands due to the symmetric and asymmetric O–C–O stretching vibrations of adsorbed formate ion are rather insensitive to the nature of the adsorbent (*5–7*)), it was not possible to decide unambiguously whether the formate ion is totally bonded to the support, or whether a part of it occupies a fraction of the Rh, nor to establish the stability of formate species on Rh.

As the formation of surface formate was also identified in the methanation of CO and CO_2 on supported Rh (*3, 8*), and it proved rather reactive at the temperatures of the above reactions, it seemed important to investigate more closely its formation and stability on clean Rh under ultrahigh-vacuum (UHV) conditions without the disturbing effect of supports. In order to have a stronger link with the real catalyst, we used first Rh foil instead of Rh single crystal.

The adsorption of formic acid has been investigated by modern surface techniques on Ni (*9, 10*), Cu (*9–15*), Ag (*9, 16*), Au (*10*), Ru (*17*), Pt (*18*), and Pb (*12, 13*) surfaces. In harmony with previous findings on supported metals (*5, 6*), at low temperatures formic acid adsorbs associatively, but at elevated temperatures the adsorption is dissociative. In some cases the presence of

---

[1] Author to whom all correspondence should be addressed.

0021-9517/83 $3.00

preadsorbed oxygen is required for the dissociative adsorption of formic acid (*9, 14*). The stability of surface formate depends on the nature of the metal, but in general it starts to decompose above 400 K. In this work we have studied the interaction of HCOOH vapour with Rh foil using Auger electron spectroscopy (AES), electron energy loss spectroscopy in the electronic energy range (ΔE = 0–30 eV), and temperature-programmed desorption. No previous work on electron energy loss spectroscopy in the electronic energy range has been reported for HCOOH on metals, although some studies have been made in the vibrational energy range (*15, 16*).

2. EXPERIMENTAL

Rh foil (3 *N*, 10 × 10 mm, and 0.127 mm thick) was obtained from Hicol Corporation. It was spot-welded between two tungsten wires which were themselves fixed to two Ta foils mounted on a crystal manipulator. The foil was heated resistively and its temperature was measured with a Chromel–Alumel thermocouple spot-welded to the edge of the foil. For low-temperature measurements the Rh sample was cooled by a Ta foil spot-welded to the backside of the sample and connected to a liquid-nitrogen-cooled stainless-steel tube.

The cleaning procedure was the same as that used before (*19–22*). It consisted of cycles of argon ion bombardment (typically 600 eV, 1×10^{-6} Torr Ar, 300 K, 3 μA for 10–30 min) and annealing at 1270 K for some minutes. The major contaminants were boron, sulfur, and carbon. After extended cleaning, the only impurity detected on the Rh surface was a small amount of boron. This could be eliminated by annealing at lower temperature, at 800 K.

HCOOH was a product of Merck. It was purified and stored in the manner reported by Madix *et al.* (*9*). The purity was tested during experiments with a quadrupole mass spectrometer. Extended vacuum evaporation at 228 K removed methanol and acetic acid impurities. Mass spectra of the purified formic acid showed only very slight evidence of H_2O as an impurity. HCOOH vapor was introduced into the chamber from an auxiliary vacuum system pumped by a small ion pump through a stainless-steel tube with a diameter of 0.8 cm. The Rh foil was positioned about 1.2 cm in front of the effusion hole. HCOOH was adsorbed at pressures between 1×10^{-8} and 1×10^{-6} Torr.

The experiments were carried out in a Varian ion-pumped UHV system which was equipped with a single-pass CMA (PHI), with a 3-grid retarding field analyzer (VG), and with a quadrupole mass analyzer. The base pressure was 1.5×10^{-10} Torr.

For electron energy loss spectra the gun of the CMA was used as a primary electron source with energies between 20 and 125 eV and a beam current of 0.2–1.0 μA (*23*). The backscattered electrons were analyzed with the CMA. A modulation voltage of 0.1 eV was found to be the optimum for the used system. The speed of taking a spectrum was 0.4 eV/s. The exact positions of the peak maxima of energy losses were determined by a Keithley electrometer. Electron energy loss spectra were taken in $dN(E)/dE$ form.

Auger spectra were taken with 3-V peak-to-peak modulation, 1–10 μA of incident current, 2.5 kV of incident energy, and a sweep rate of 3 V/s.

3. RESULTS

3.1. Adsorption at 300 K

3.1.1. Auger studies. An attempt was made to follow the adsorption of HCOOH by recording Auger spectra of Rh as a function of its exposure to HCOOH.

The Auger spectrum of a clean Rh surface is shown in Fig. 1. Exposure of the clean surface to HCOOH at 300 K resulted in the appearance of C and O KLL signals at 272 and 514 eV. At the same time, mass spectrometric analysis of the gas phase indicated H_2, H_2O, and CO_2 formation; their

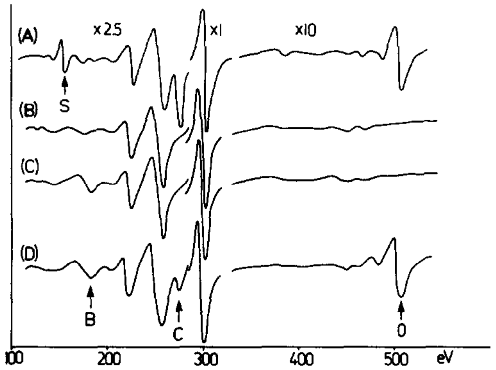

FIG. 1. Auger spectra of the Rh surface taken: (A) before cleaning, (B) after argon ion bombardment and heating to 800 K, (C) after argon ion bombardment and heating to 1300 K, (D) after exposure to 60 L HCOOH at 300 K.

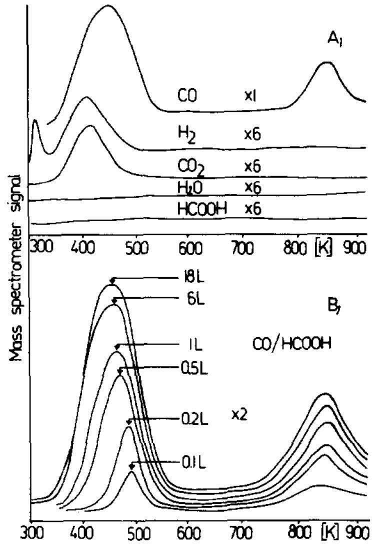

FIG. 2. (A) Thermal desorption spectra following HCOOH adsorption (60 L) on a clean Rh surface at 300 K. The curves are uncorrected for detection sensitivities. (B) Thermal desorption spectra of CO following HCOOH adsorption of different exposures.

amounts were larger than that corresponding to the fragmentation of HCOOH due to the electron beam. However, no CO evolution was observed during the adsorption. (In these measurements, the sample was in front of the analyzer head of the mass spectrometer (MS) during the admission of HCOOH.) The O signal was found to be sensitive to the beam; even at low beam current it decreased appreciably with the duration of the beam exposure. The carbon signal behaved differently as a slight increase occurred in its intensity during the beam exposure. A similar phenomenon was found during the adsorption of CO on the Rh(110) surface (*24*). On the basis of the changes of carbon and oxygen Auger signals, a saturation coverage was reached at 10–12 L HCOOH exposure.

3.1.2. Thermal desorption studies. Thermal desorption spectra were taken at a linear heating rate of 13 K s^{-1}. The main product of desorption is CO; it desorbs in two stages (Fig. 2).

The peak temperature of the low-temperature stage was shifted from ~500 K to 447 K with increase of the coverage (Fig. 2). The desorption maximum of the high-temperature stage was practically constant (~830 K) at different HCOOH exposures.

Smaller amounts of H_2 and CO_2 were also desorbed; desorption maxima of H_2 were observed at ~310 K and at 408 K, and that of CO_2 at 412 K. There was no detectable desorption of HCOOH, H_2O, or the HCOO radical.

The kinetic data for the thermal desorption calculated by the different methods are listed in Table 1, which also contains the data for the desorption of CO from various Rh surfaces. It appears that the activation energy values for the desorption of CO following the adsorption of HCOOH are in good agreement with those obtained after the adsorption of CO on Rh surfaces (*19, 20, 22, 24–27*).

Following the thermal desorption measurements, the Auger spectrum indicated that only small amounts of carbon and oxygen remained as impurities on the surface.

We should point out that we also observed a high-temperature desorption peak of CO (Fig. 2) following the adsorption of HCOOH on the Rh surface. The temperature of desorption of CO in this stage was somewhat lower than that found by Sexton and Somorjai (*19*) after treating the Rh foil

TABLE 1

Summary of the Results of Thermal Desorption Measurements on Rh

State[a]	Adsorption temp. (K)	Form of orientation of Rh	$T_{\max}$ (K)	E[b] (kJ/mol)	E[c] (kJ/mol)	Ref.
HCOOH/HCOOH	95	Foil	153	38		This work
HCOOH/HCOOH	95	Foil	172	43		This work
CO_2/HCOOH	95	Foil	275–295	$\sim$72		This work
CO_2/HCOOH	95, 300	Foil	412	103		This work
H_2/HCOOH	95	Foil	275–295	$\sim$72		This work
H_2/HCOOH	95, 300	Foil	408	102		This work
H_2O/HCOOH	95	Foil	300	75		This work
CO/HCOOH	300	Foil	447–490	118		This work
			830	208		This work
CO/CO	300	Foil	458–495	124		(*27*)
CO/CO	300	Wire	500	134		(*22*)
CO/CO	300	Foil	523	133		(*19*)
CO/CO	300	(110)	500	130		(*24*)
CO/CO	300	(111)	470–490		132	(*25*)
CO/CO	300	(110)		129		(*20*)
CO/CO	300	(111)		121		(*20*)
CO/CO	300	Tip	485–530	132		(*26*)

[a] The notation of A/B refers to desorption peak for gas A following adsorption of gas B.

[b] Calculated from the observed values of $T_{\max}$ with a preexponential factor of 10^{13} s^{-1}.

[c] Calculated from peak width and the temperature at which the maximum rate of desorption occurs.

with CO, H_2 + CO, and H_2 + CO_2 mixtures. No such desorption peak for CO was registered, however, after adsorption of CO alone on a clean Rh surface (*27*).

3.1.3. Electron energy loss studies. Before determination of the electron energy loss (EEL) spectrum of adsorbed HCOOH, we investigated the dependence of the elastic peak height reflected from a clean Rh foil on the primary energy at 20–110 eV. As Fig. 3A shows, the maximum reflectance appeared slightly below 70 eV.

The EEL spectrum of clean Rh foil is shown in Fig. 3B. The characteristic loss energies of a Rh foil occurred at 4.1, 5.4, 19.6, and 29.5 eV; these losses showed little variation with the primary electron energy. It should be noted that on a carefully cleaned Rh surface (bombardment with argon ions and subsequent heat treatment at 800 K) we did not find the loss detected at 7.9–8.6 eV by previous authors (*28–30*). We did observe losses at 7.3–9.5 eV, how-

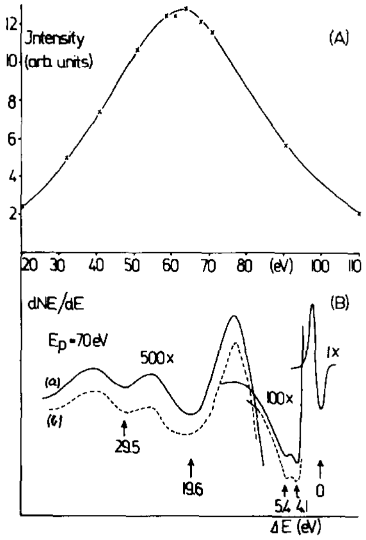

FIG. 3. (A) Dependence of the elastic peak height reflected from a clean Rh foil on primary energies. (B) The electron energy loss spectrum of Rh foil after argon ion bombardment and annealing at 1270 K (a) and at 800 K (b). No Auger signal due to boron was detected in the latter case.

ever, when the surface was contaminated by oxygen or nitrogen (*27*).

Further measurements were performed at a primary electron energy of 70 eV. In this case the beam current was 0.2 μA and the modulation voltage 0.1 eV.

Exposure of the clean Rh surface to HCOOH at 300 K enhanced the intensity of the elastic peak; the shape of the broad loss at 4.1–5.4 eV became "sharp," with peaking at 4.6 eV. The intensity of the 19.6-eV loss decreased, this occurring with the loss at 29.5 eV. The adsorption of HCOOH resulted also in the appearance of new losses, at 13.2 and 9.5–9.9 eV (Fig. 4A). Their intensities increased up to an exposure of 12 L HCOOH. However, when the measurements were performed directly after HCOOH adsorption (1 min), an intense loss peak appeared at 11.3 eV and a less intense one at 13.2 eV (Fig. 4B). The intensity of the 11.3-eV loss rapidly decreased, while a loss feature developed at 9.5–9.9 eV and the intensity of the 13.2-eV loss was also enhanced. The loss at 11.3 eV had completely disappeared after 5–8 min.

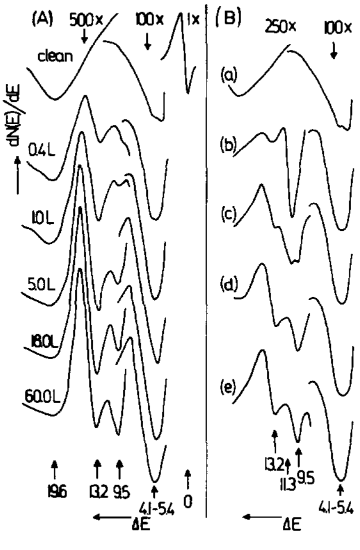

FIG. 4. (A) Electron energy loss spectra of Rh surface as a function of HCOOH exposure at 300 K. (B) Electron energy loss spectra of Rh foil exposed to 30 L HCOOH at 300 K taken after 0.5 min (b), 4 min (c), 8 min (d), and 11 min (e). Spectrum of clean sample before HCOOH adsorption (a).

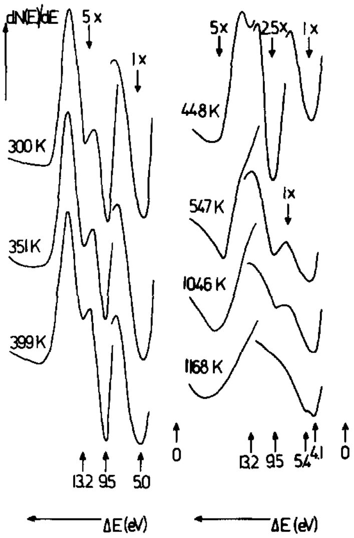

FIG. 5. Electron energy loss spectra taken after heating the Rh foil exposed to 60 L HCOOH to different temperatures. Heating rate was ~13 K s^{-1}. Heating time at a given temperature was ~4 min.

The EEL spectra taken after heating of the sample (exposed to 60 L HCOOH) to different temperatures are shown in Fig. 5. It appears that the stable new losses (13.2 and 9.5 eV) behave differently. While the intensity of the 13.2-eV loss gradually decreases from 350 K, and disappears above 445 K, the intensity of the loss at 9.5 eV increases up to ~600 K, and decreases only above this temperature. At 544 K a shift occurs in the 19.6-eV loss. The EEL spectrum of "clean" Rh appears only after heating of the sample to 1165 K.

Table 2 gives the loss energies observed in the present work.

3.2. Adsorption at 95 K

3.2.1. Thermal desorption studies. The adsorption of HCOOH was also investigated at low temperature, 95 K. Figure 6 shows the desorption spectra of HCOOH following HCOOH adsorption at 95 K. No, or only extremely slight, HCOOH desorption was observed below 0.6 L exposure.

TABLE 2

Characteristic Electron Energy Losses of Rh Surface Covered with Different Adsorbates

Adsorbates	Losses (eV)								
Clean metal	4.1	5.4						19.6	29.5
HCOOH at 95 K			8.2		11.3		14.2–14.8		
HCOOH at 300 K				9.5		13.2			
CO at 300 K						13.2			
O_2 at 300 K				9.5					
CO_2 at 95 K							14.2		
CO_2 at 300 K				9.5		13.2			
H_2O at 95 K (multilayer)			8.6				14.4		

An initial peak occurred at 172 K and grew with exposure until 6 L. A second peak was observed at 153 K. This peak did not saturate with exposure. Great attention was paid to detect any formation of H_2O. A signal at 18 amu was observed, however, only at the desorption temperature of HCOOH. The ratio of 18/46 amu (1.12) agreed very well at every exposure with that established in the mass spectrometric analysis of HCOOH, so we may conclude that no H_2O formation occurred during the adsorption/desorption of HCOOH on Rh below 200 K.

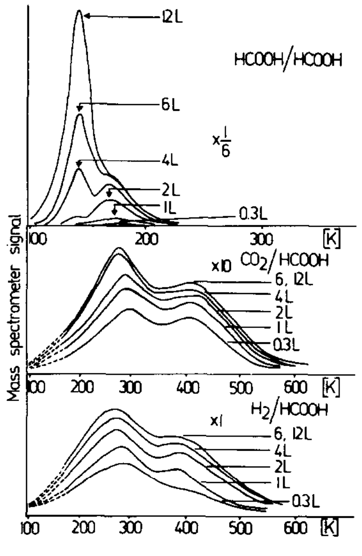

FIG. 6. Thermal desorption spectra following HCOOH adsorption on Rh surface at 95 K. The HCOOH exposure was 60 L. The curves are uncorrected for detection sensitivities.

The formation of H_2O was detected, however, above 200 K; T_{max} = 290–305 K. Desorption of H_2 and CO_2 occurred in the same temperature ranges with the peak maxima at 275–295 K and ~410 K. Taking into account the sensitivity of the mass spectrometer used and the pumping speed of the gases, we obtain values of 8.3 for the H_2/CO_2 and 3.3 for the H_2/H_2O ratios. We again observed a significant CO desorption; T_{max} = 457–500 K and 830 K. The amount of CO desorbed agreed well with that found after adsorption of HCOOH at 300 K. The ratios for CO/H_2O and CO/CO_2 were calculated to be 4.5 and 10.9.

We note here that a very weak signal at 16 amu (CH_4) was also observed at 350–400 K. Attempts to increase its intensity, however, were not successful.

3.2.2. Electron energy loss studies. Exposure of the clean surface to HCOOH at 95 K produced a different EEL spectrum from that obtained at 300 K. At very low exposure (0.15–0.5 L) a new loss appeared at 11.3 eV. With increase of exposure it became more intense and, at the same time, losses developed at 14.2–14.8 and 8.2 eV

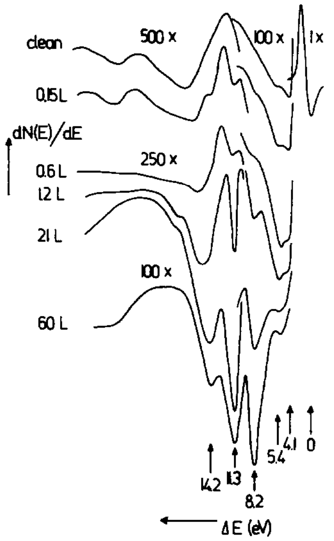

FIG. 7. Electron energy loss spectra of Rh foil as a function of HCOOH exposure at 95 K.

(Fig. 7). The intensities of the losses at 8.2 and 14.2–14.8 eV decreased rapidly with the rise of temperature and disappeared at 200 K. The loss at 11.3 eV decreased gradually and it disappeared around 300 K (Fig. 8). Similarly to that observed after adsorption of HCOOH at 300 K, the occurrence of this loss was found to be very sensitive to the experimental conditions applied. When the sample exposed to HCOOH at 95 K was heated directly to a selected temperature and, after 30–60 s, cooled quickly to 95 K, the 11.3-eV loss was detected even after warming the sample to 330 K. Extending the time of keeping the sample at 275–300 K for 3–10 min caused the reduction and finally the elimination of this loss.

A new loss at 13.2 eV began to develop at 190 K. The intensity of this loss increased up to about 300 K, remained practically constant up to 380 K, then decreased and was eliminated only at 513 K. Another new loss around 9.5 eV could be identified above 200 K; its intensity increased with the temperature and was eliminated only above 1150 K. These changes are illustrated in Fig. 9, where the intensities of the losses are plotted as a function of thermal treatment.

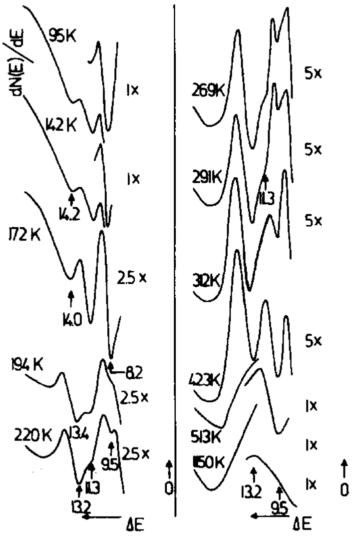

FIG. 8. Electron energy loss spectra taken after heating the sample exposed to 60 L HCOOH at 95 K to different temperatures. Heating rate was ~13 K s^{-1}. The heating time at a given temperature was ~4 min.

4. DISCUSSION

4.1. Electron Energy Loss Measurements

The EEL spectrum of Rh has been investigated by a number of authors. Losses were found at 7.9–8.1 (*28, 31, 32*), 8.6–9 (*29–32, 34*), 24.6–26 (*28, 30*), and 32.5–35 eV (*30–34*).

In our measurements on carefully cleaned Rh surfaces, we observed losses at

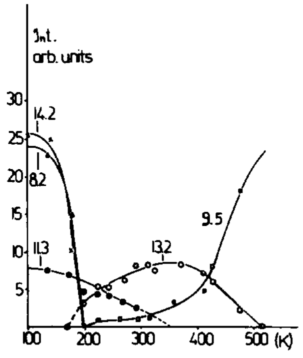

FIG. 9. Changes in the intensities of new losses caused by the adsorption of HCOOH at 95 K after heating the sample to different temperatures.

4.1, 5.4, 19.6, and 29.5 eV. The positions of these losses remained unaltered at primary energies of 40–100 eV. The basic difference between the loss spectra obtained in this work and previous ones is that we have not detected any loss features at 8.6–9 and 7.9–8.1 eV. The possible reasons for the different results will be discussed in detail in a subsequent paper (*27*). We note here, however, that in the majority of the previous measurements the vacuum conditions were poorer than in the present case, and the sample cleanliness was not checked by Auger spectroscopy in either work. Accordingly, we are inclined to think that in the previous studies the Rh samples were not sufficiently clean and the losses observed at 8.6 and at 7.9 eV might have been caused by surface contaminants.

The adsorption of HCOOH on clean metal surfaces has not previously been investigated by EEL spectroscopy.

The adsorption of HCOOH on a clean Rh surface produced basically different EEL spectra at 95 and 300 K. While for low-temperature adsorption new losses appeared at 14.2–14.8, 11.3, and 8.2 eV, for the high-temperature adsorption the main losses were at 13.2 and 9.5 eV. These results indicate that completely different surface species exist on the surface at 95 and 300 K.

As a starting point we may assume that at low temperature molecularly and/or dissociatively bonded HCOOH are the dominant surface species, while at 300 K these surface species may have decomposed further.

In order to interpret the results of the EEL spectra of adsorbed HCOOH, it seemed necessary to investigate the loss spectra of the possible products of the decomposition of HCOOH. This work will form the subject of a separate publication (*27*); here we mention only the main characteristics, which are shown in Table 2.

The adsorption of CO caused an intense loss at 13.2 eV in good agreement with the data obtained on other metals (*23, 35, 36*). This may indicate that electron transitions occur within the adsorbed CO between levels which are only little influenced by the metal. Accordingly, the appearance of the 13.2-eV loss following the adsorption of HCOOH belongs, no doubt, to the formation of adsorbed CO as a result of the reaction in the adsorbed layer.

The 13.2-eV loss feature was also observed when CO_2 was adsorbed on Rh at 300 K; in addition a weak loss at 9.5–9.9 eV was also registered. As this latter loss was identified during the adsorption of O_2, we may conclude that at least a part of CO_2 adsorbs dissociatively on Rh at 300 K yielding adsorbed CO and O. This result is in harmony with those obtained on a Rh(111) surface using HREEL (vibration) spectroscopy (*37, 38*).

While at 300 K there was no indication in the EEL spectra for the presence of any other loss attributable to the adsorbed CO_2; at 95 K the adsorption of CO_2 caused a very weak loss at 14.2 eV. The intensity of this loss decreased markedly when the temperature was raised and was completely eliminated at 230 K without producing a loss at 13.2 eV. This indicates that the CO_2 adsorbs weakly on Rh at lower temperature and it desorbs entirely below its dissociation temperature on Rh. The adsorption of H_2O on Rh also produced a loss at 14.4 eV and a weak loss at 8.6 eV at higher exposures, when a multilayer of H_2O was formed.

Taking into account the results and the conclusions of the thermal desorption measurements (see later), and that the losses observed following the adsorption of either CO_2 or H_2O appeared at much higher exposures, we may conclude that the losses observed after HCOOH adsorption at 95 K belong exclusively to the adsorbed HCOOH. The contribution of the decomposition products of adsorbed HCOOH to these losses is minimal, if any.

On the basis of the behaviour of the losses, we assume furthermore that the loss at 8.2 eV belongs to the molecularly adsorbed HCOOH and that at 11.3 eV to the formation of formate ions. The following observations seem to support this proposal.

The EEL spectrum of HCOOH has been recently published by Ari and Hasted (*39*). The dominant feature in the EEL spectrum was a loss at 8.36 eV in the range 7–12 eV. In the vacuum ultraviolet absorption spectrum of formic acid a strong absorption band appeared at 159 nm (7.8 eV) (*40*).

This band was assigned to the first π–π^* transition band. The band has a mixed character of a local excitation within the C=O group and charge transfer-type excitation accompanied by an electron transfer from the electron donor (OH) to the electron acceptor (C=O) group.

In order to clarify the origin of the 11.3-eV loss, the adsorption of HCOOH on Cu(111) was investigated by EEL spectroscopy (*41*). It is known that HCOOH adsorbs dissociatively on Cu surfaces and the formate ion is stable up to 400 K. Adsorption of HCOOH on a clean Cu(111) surface at 300 K produced only an intense loss at 11.3 eV in the EEL spectrum (*41*). It is very likely that this loss is due to the formate ion as neither CO nor CO_2 adsorbs on a clean Cu(111) surface at 300 K (*43–47*).

The origin of the loss at 14.2–14.8 eV is not yet clear. As its intensity became larger when the HCOOH multilayer developed and it changed in parallel with that at 8.2 eV when the sample was heated (Figs. 8, 9), we tentatively attribute this loss also to the molecularly adsorbed HCOOH.

In support of this assumption we may mention that Peyerimhoff and Buenker (*42*) in their theoretical comparison of formic acid and formate ion concluded that although the electronic spectra are quite similar through their first six excited states, the $^{3,1}B(^{3,1}B_1)$ pair possesses a much larger (by 3.5 ev) transition energy in the acid than in the unprotonated species.

4.2. Interaction of HCOOH with Rh Surface

The thermal desorption spectra of formic acid following the adsorption at 95 K indicate that HCOOH adsorbs strongly and dissociatively on the Rh up to 0.6 L:

$$HCOOH_{(g)} = HCOOH_{(a)}, \qquad (1)$$

$$HCOOH_{(a)} = HCOO_{(a)} + H_{(a)} \qquad (2)$$

(appearance of the loss at 11.3 eV).

Further exposure resulted in a desorption peak at 172 K and the appearance of the losses at 8.2 and 14.2–14.8 eV attributed to the weakly adsorbed HCOOH. The development of a low-temperature peak at 153 K, which did not saturate with exposure, suggests multilayer condensation of HCOOH. The desorption of weakly held HCOOH,

$$HCOOH_{(a)} = HCOOH_{(g)} \qquad (3)$$

is complete at 200 K. This is also the temperature at which the 14.2- and 8.3-eV losses are no longer discernible. We can assume that the processes

$$HCOO_{(a)} + H_{(a)} = HCOOH_{(a)} = HCOOH_{(g)} \qquad (4)$$

also contribute, at least to a small extent, to the desorption of HCOOH.

The decomposition of formate ion starts around 200 K. The reaction is quite complex, at higher temperatures, and some side reactions (e.g., dissociation of CO_2) also occur influencing the product distribution, so the decomposition of formate ion cannot be characterized by just one or two simple equations. In the temperature range of 200–300 K, H_2, H_2O, and CO_2 evolution was observed. The peak temperatures of desorption for H_2 and CO_2 were practically the same as those observed after the adsorption of H_2 and CO_2 at the same coverages (*27*). From this agreement, we can only conclude that the activation energy for the decomposition of formate ion in this temperature range is not higher than that for the desorption of H_2 and CO_2 (Table 1). It is very likely that the same is valid for the formation of H_2O in this temperature range.

The decomposition of surface formate was accompanied by a gradual decrease in the intensity of the 11.3-eV loss and with the appearance of a 13.2-eV loss. This indicates that in the decomposition process, chemisorbed CO is also formed, the desorption of which, however, occurred at much higher temperature, above 400 K. As the peak temperature and the activation energy of the desorption of CO agreed well with the values determined after CO adsorption on Rh surfaces, we may conclude that the formation of gaseous CO is a desorption rate-limited process.

Simultaneously with the appearance of the 13.2-eV loss around 200 K due to chemisorbed CO, a loss at 9.5 eV was also detected (Figs. 5 and 8), with a growing intensity at higher temperatures. This loss no doubt belongs to the formation of the chemisorbed oxygen (Table 2).

Accordingly, in addition to the processes

$$HCOO_{(a)} = H_{(a)} + CO_{2(a)}, \quad (5)$$

$$2H_{(a)} = H_{2(g)}, \quad (6)$$

$$CO_{2(a)} = CO_{2(g)}, \quad (7)$$

the reaction

$$HCOO_{(a)} = H_{(a)} + CO_{(a)} + O_{(a)} \quad (8)$$

also occurs on the Rh surface at 200–300 K, similar to observations on Fe and W surfaces (*48, 49*). We can also assume that similar to that observed on supported Rh (*1–4*) the dissociation of adsorbed CO_2 (possibly promoted by hydrogen),

$$CO_{2(a)} = CO_{(a)} + O_{(a)}, \quad (9)$$

can also contribute to the formation of chemisorbed CO and O. The formation of H_2O is very probably the result of the reaction between adsorbed hydrogen and oxygen,

$$2H_{(a)} + O_{(a)} = H_2O_{(a)} = H_2O_{(g)}. \quad (10)$$

Thermal desorption measurements, however, show that the surface reaction is possibly not complete in this temperature range, as evolution of both H_2 and CO_2 was also observed at higher temperatures, $T_{max} \approx 400$ K. As no such desorption peaks were noticed following either H_2 or CO_2 adsorption over Rh it appears that both H_2 and CO_2 productions are reaction rate limited in this temperature range, and very likely the result of the decomposition of a more stable formate species. This is in harmony with the observation that the weak loss at 11.3 eV can be detected even after heating the sample exposed to HCOOH to 300–330 K for only 1–4 min (Fig. 4).

The decomposition of formate in this temperature range produces mainly H_2 and CO_2 (Eqs. (5)–(7)), as no increase in the intensity of the 13.2-eV loss can be noticed above 300 K. The desorption of CO is negligible below 400 K. The increase in the intensity of the 9.5-eV loss apparently indicates that reaction (8) occurs in this temperature range, too. However, the more detailed study of the interaction of O_2 with Rh revealed that the intensity of the 9.5-eV loss is strongly affected by the reaction of oxygen with the Rh, i.e., by the diffusion of oxygen into the surface layer of Rh and by the formation of Rh-oxide, and it cannot be related directly to the changes of the surface concentration of chemisorbed oxygen (*27*).

The concentration of this more stable surface formate is, however, very low and it decomposes rapidly at even slightly above room temperature under isothermal conditions. This is well illustrated by the results obtained by keeping the sample (exposed to HCOOH at 300 or 95 K) at 300–330 K for a more extended time (for more than 4 min), when the 11.3-eV loss could no longer be detected and the amount of H_2 + CO_2 evolved in the subsequent thermal desorption significantly decreased.

Taking into account the amount of CO formed and its ratio to other products, as well as the amount of H_2 and CO_2 evolved in the high-temperature stage (which even in the optimal case does not exceed one-quarter of that formed in the low-temperature range), it appears that only less than 10% of formate groups decompose in the high-temperature stage. This surface concentration can be further reduced by keeping the sample at 300–330 K for 4–10 min.

The results unambiguously show that in contrast to the previous belief (see discussion in Ref. (*2*)) the formate ion is unstable over Rh, and decomposes almost completely around room temperature. This conclusion is valid not only for the low pressure range, but also at the elevated pressures on supported Rh. Adsorption of 10 Torr HCOOH on Rh/SiO_2 at 140 K produced strong bands at 1595 and 1370 cm^{-1} in the infrared spectrum, indicative of the dissociative adsorption of HCOOH; these bands, however, were completely eliminated when the sample was heated to higher temperatures (250–290 K). Note that no such bands appeared in the absence of Rh, i.e., on silica alone.

All these results support our former conclusion that the formate ion formed in any of the following reactions: adsorption of HCOOH (*1*), surface interaction between H_2 and CO_2 (*1, 2*), methanations of CO (*3*) and CO_2 (*4, 8*) in the temperature range of 325–573 K on alumina, magnesia, and titania-supported Rh, is located not on the Rh but exclusively on the supports. In the light of its instability it is also conceivable that the formate ion formed on the support itself in the reaction of chemisorbed CO_2 (hydrocarbonate) and hydrogen which, having been activated on Rh, had then migrated onto the support. This is in harmony with our recent observation that no losses characteristic for the adsorbed HCOOH were detected by EEL spectroscopy during the co-adsorption of $H_2 + CO_2$ on a clean Rh surface at 100–350 K (*27*). The dissociation of CO_2, however, was greatly enhanced in the presence of hydrogen (*27*).

REFERENCES

1. Solymosi, F., Erdöhelyi, A., and Kocsis, M., *J. Catal.* **65,** 428 (1980).
2. Solymosi, F., Erdöhelyi, A., and Bánsági, T., *J. Chem. Soc. Faraday Trans. 1* **77,** 2645 (1981).
3. Solymosi, F., Tombácz, I., and Kocsis, M., *J. Catal.* **75,** 78 (1982).
4. Solymosi, F., and Erdöhelyi, A., *in* "Proceedings, 7th International Congress on Catalysis, Tokyo, 1980," p. 1448. Elsevier, Amsterdam, 1981.
5. Hair, M. L., "Infrared Spectroscopy in Surface Chemistry." Dekker, New York, 1967.
6. Mars, P., Scholten, J. J. F., and Zwietering, P., *in* "Advances in Catalysis" (D. D. Eley, H. Pines, and P. B. Weisz, Eds.), Vol. 14, p. 35. Academic Press, New York, 1963.
7. Trillo, J. M., Munuera, G., and Criado, J. N., *Catal. Rev.* **7,** 51 (1972).
8. Solymosi, F., Erdöhelyi, A., and Bánsági, T., *J. Catal.* **68,** 371 (1981).
9. (*a*) Madix, R. J., *in* "Advances in Catalysis," Vol. 29, p. 1. Academic Press, New York, 1980; (*b*) McCarty, J., Falconer, J., and Madix, R. J., *J. Catal.* **30,** 235 (1973).
10. Joyner, R. W., and Roberts, M. W., *Proc. R. Soc. London Ser. A* **350,** 107 (1976).
11. Au, C. T., Breza, J., and Roberts, M. W., *Chem. Phys. Lett.* **66,** 340 (1979).
12. Roberts, M. W., *Chem. Soc. Rev.* **6,** 373 (1977).
13. Isa, S. A., Joyner, R. W., Mataloob, M., and Roberts, M. W., *Appl. Surf. Sci.* **5,** 345 (1980).
14. Roberts, M. W., *in* "Advances in Catalysis," Vol. 29, p. 55. Academic Press, New York, 1980.
15. Sexton, B. A., *Surf. Sci.* **88,** 319 (1979).
16. Sexton, B. A., and Madix, R. J., *Surf. Sci.* **105,** 177 (1981).
17. Larson, L. A., and Dickinson, J. T., *Surf. Sci.* **84,** 17 (1979).
18. Steinbach, F., and Hansen, V., *Surf. Sci.* **62,** 504 (1977).
19. Sexton, B. A., and Somorjai, G. A., *J. Catal.* **46,** 167 (1977).
20. Castner, D. G., Sexton, B. A., and Somorjai, G. A., *Surf. Sci.* **71,** 519 (1978).
21. Castner, D. G., Dubois, L. H., Sexton, B. A., and Somorjai, G. A., *Surf. Sci.* **103,** L134 (1981).
22. Campbell, C. T., and White, J. M., *J. Catal.* **54,** 289 (1978).
23. Solymosi, F., and Kiss, J., *Surf. Sci.* **108,** 641 (1981).
24. Marbow, R., and Lambert, R. M., *Surf. Sci.* **67,** 489 (1977).
25. Thiel, P. A., Williams, A. D., Yates, J. T., and Weinberg, W. H., *Surf. Sci.* **84,** 54 (1979).
26. Gorodetskii, V. V., and Nieuwenhuys, B. E., *Surf. Sci.* **105,** 299 (1981).
27. Solymosi, F., and Kiss, J., to be published.
28. Lynch, M. J., and Swan, J. B., *Aust. J. Phys.* **21,** 811 (1968).
29. Pierce, D. T., and Spicer, W. E., *Phys. Status Solidi B* **60,** 689 (1973).
30. Staib, P., and Ulmer, K., *Z. Phys.* **219,** 381 (1969).
31. Cox, J. T., Hass, G., and Hunter, W. R., *J. Opt. Soc. Amer.* **61,** 360 (1971).

32. Seignac, S., and Robin, S., *C. R. Acad. Sci. (Paris) Ser. B* **271,** 919 (1970).
33. Weaver, J. H., *Phys. Rev. B* **11,** 1416 (1975).
34. Weaver, J. H., Olson, C. G., and Lynch, D. W., *Phys. Rev. B* **15,** 4155 (1977).
35. Netzer, F. P., and Matthew, J. A. D., *Surf. Sci.* **51,** 352 (1975).
36. Menzel, D., Hesse, R., Staib, P., and Menzel, D., *Appl. Phys.* (Germany) **18,** 227 (1979).
37. Dubois, L. H., and Somorjai, G. A., *Surf. Sci.* **91,** 514 (1980).
38. Dubois, L. H., and Somorjai, G. A., *Surf. Sci.* **88,** L13 (1979).
39. Ari, T., and Hasted, J. B., *Chem. Phys. Lett.* **85,** 153 (1982).
40. Nagakura, S., Kaya, K., and Tsubomura, H., *J. Mol. Spectrosc.* **13,** 1 (1964).
41. Solymosi, F., and Kiss, J., unpublished results.
42. Peyerimhoff, S. D., and Buenker, R. J., *J. Chem. Phys.* **50,** 1846 (1969).
43. Solymosi, F., and Kiss, J., *Surf. Sci.* **104,** 181 (1981).
44. Solymosi, F., and Kiss, J., *Surf. Sci.* **108,** 368 (1981).
45. Papp, H., and Pritchard, J., *Surf. Sci.* **53,** 371 (1975).
46. Kessler, J., and Thieme, F., *Surf. Sci.* **67,** 405 (1977).
47. Wachs, J. E., and Madix, R. J., *J. Catal.* **53,** 208 (1978).
48. Benziger, J. B., and Madix, R. J., *J. Catal.* **65,** 49 (1980).
49. Benziger, J. B., Ko, E. I., and Madix, R. J., *J. Catal.* **58,** 149 (1979).